Stable stationary vortices and traveling oscillatory vortices in a stenotic fluid-flow channel

David W. Pravica,[1] Martin Bier,[2] Robert S. Brock,[2] and Orville W. Day, Jr.[2]
[1]*Department of Mathematics, East Carolina University, Greenville, North Carolina 27858, USA*
[2]*Department of Physics, East Carolina University, Greenville, North Carolina 27858, USA*
(Received 30 June 2005; published 20 December 2005)

A shearing zonal flow of viscous fluid near a boundary perturbation can generate vortices that either remain attached near the boundary or detach to be abruptly carried downstream. At low speed a stationary attached vortex develops downstream from the perturbation. At higher speeds an array of traveling vortices forms, with successive rolls rotating in opposite directions. This report presents a quantitative explanation of vortex generation. We consider a setup that leads to a straightforwardly analyzable, Schrödinger-type equation. In the case of bloodflow through arteries the aforementioned traveling vortices are detectable as oscillations in the 1–100 Hz range. The detection of such oscillations is simple and is used to diagnose arterial stenosis.

DOI: 10.1103/PhysRevE.72.067303 PACS number(s): 47.32.−y, 47.27.Cn, 47.60.+i, 87.19.Uv

Numerous studies have examined the genesis and evolution of vortices near a bluff body or boundary perturbation. There remains an interest in understanding vortex streets, turbulence and noise in fast moving fluids for applications to astronomy, engineering and medicine [1–3]. Numerical modeling of pulsatile flow in arteries reveals qualitative differences between harmonically-forced flows and the unidirectional flow produced by the heart. Indeed, Liao *et al.* [4] have shown that since the aortic heart valve acts as a diode to the flow, new vortices can only travel downstream from a boundary perturbation. These fluid disturbances, when acting inside a distensible tube, will create traveling pressure waves that hold important information on the arterial-boundary perturbation [5].

In this paper we study 2D laminar flow through an analytic narrowing (stenosis) in a channel. We analyze a setup that, depending on parameter values, exhibits stationary as well as traveling vortices. Stationary vortices remain attached to the stenosis. Traveling vortices flow down the channel and form an oscillatory "street." The key step in our analysis is the transformation of the fluid equations to a Schrödinger-type equation. Subsequent spectral analysis then reveals both the traveling and the stationary vortices. We derive conditions for the occurrence of both types of vortices in terms of geometry, boundary shear stress and Reynolds number. We will show that a sufficiently large boundary vorticity layer is required for stationary vortices and that a sufficiently high Reynolds number with a boundary shear stress is required for traveling oscillatory solutions.

We consider 2D, viscous, incompressible, quasi-uniform vorticity flow [1],

$$\partial_t \omega + \partial(\psi,\omega)/\partial(x,y) = \nu_0 \Delta_{x,y}\omega, \tag{1}$$

$$\Delta_{x,y}\psi \equiv \partial_x^2\psi + \partial_y^2\psi = \omega, \tag{2}$$

where ν_0 is the kinematic viscosity. The velocity field $\vec{q}=(u,v)$ is computed from the stream function $\psi(x,y,t)$ as $u(x,y,t)=-\partial_y\psi$ and $v(x,y,t)=\partial_x\psi$ [6]. The stream-vorticity Jacobian in Eq. (1) is defined as

$$\partial(\psi,\omega)/\partial(x,y) = \partial_x\psi\partial_y\omega - \partial_y\psi\partial_x\omega = \vec{q}\cdot\nabla\omega. \tag{3}$$

The (complex) flow domain is

$$\mathcal{D}_{x,y} \equiv \{x+iy: -\infty < x < \infty, |\eta(x,y)| < 1\}, \tag{4}$$

where $\eta(x,y)$ is a harmonic function, defined below.

To simplify the flow domain, consider the conformal transformation from $z=x+iy$ to $\zeta=\xi+i\eta$, defined by

$$\zeta(z) = \frac{z}{h}\exp\left[-\frac{m}{1+z^2/p^2}\right], \tag{5}$$

which is singular only for $(x,y)=(0,\pm p)$. If $h>0$ is the half-width of the channel, then for $m<0$, $|\eta|<1$ and $|y|<p$, the region contains a single pair of bumps (stenoses) near the origin, located at $(x,y)=(0,\pm y_0)$ where

$$y_0 = h\exp[-|m|p^2/(p^2-y_0^2)]. \tag{6}$$

In the case of shallow perturbations, $p \gg y_0$, we can use the approximation $y_0 \simeq he^{-|m|} \simeq \kappa p^2/(6|m|)$, where κ is the curvature of the perturbation at $(x,y)=(0,\pm y_0)$. An examination of the boundary geometries in Fig. 1 shows that $2h$ is the width of the channel, and m and p set the depth and the broadness of the stenosis, respectively.

In Ref. [4] a simple Gaussian "hump" was put inside a cylindrical tube. The resulting equations were such that they could only be studied numerically. Our "Gaussian inspired" conformal transformation (5) may appear more complicated. However, after carrying simple laminar flow through this transformation, we will face analytically manageable equations. Unlike the ones in [4], our boundaries return to the reference width, $|y|=h$, at finite positions, cf. Fig. 1. The transformation (5) has a Jacobian $J \equiv \partial(\xi,\eta)/\partial(x,y)$ given by

$$\frac{1}{J} = \frac{h^2|p^2+z^2|^4\exp\left[\dfrac{2mp^2(p^2+x^2-y^2)}{|p^2+z^2|^2}\right]}{|p^4+2(1+m)p^2z^2+z^4|^2}. \tag{7}$$

So J is real-analytic in both the x and y coordinates, and $J=h^2+\mathcal{O}(|x|^{-2})$ as $|x|\to\infty$. The Jacobian J is used to transform the operators in Eqs. (1) and (2) as follows:

$$\vec{q}\cdot\nabla\omega = J\frac{\partial(\psi,\omega)}{\partial(\xi,\eta)}, \quad \Delta_{x,y} = J\Delta_{\xi,\eta}. \tag{8}$$

From Eqs. (4) and (5), the new channel region, $\mathcal{D}_{\xi,\eta}$, has width 2, defined so that $-\infty<\xi<\infty$ and $-1<\eta<1$. With the

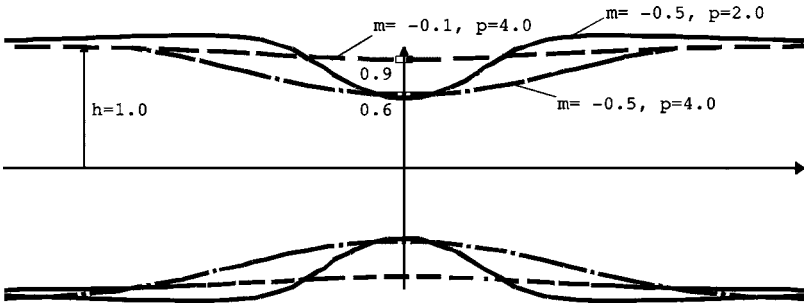

FIG. 1. The shape of the channel boundaries $\eta(x,y)=\pm 1$ in the original domain, $\mathcal{D}_{x,y}$, for the cases of stenosis $m<0$ with semichannel width $h=1.0$.

geometry simplified, a spectral analysis over the flow domain becomes an easier problem to handle.

Vorticity, which is a measure of local rotation in the fluid, is assumed to be immersed in a zonal flow with mean speed U_0. The Reynolds number is defined as $R_0=hU_0/\nu_0$. We look for a simple-harmonic vortex time response, with angular frequency $\nu_0\lambda$ (similar to the pressure amplitude p_0 in equation (12.26) of [3]), and include an exponential-translation factor:

$$\omega(x,y,t)=e^{i\nu_0\lambda t}e^{(R_0/2)\xi}W(\xi,\eta,t). \tag{9}$$

The vorticity amplitude $W(\xi,\eta,t)$ vanishes very quickly along the channel $|\xi|\to\infty$ and is assumed to be a sufficiently smooth function on $\mathcal{D}_{\xi,\eta}\times[0,T]$ for some time period $T>0$. Substituting (9) into Eq. (1) gives the equation for the vorticity amplitude,

$$\frac{1}{\nu_0 J}\frac{\partial W}{\partial t}+\frac{i\lambda}{J}W-\Delta_{\xi,\eta}W = \frac{-e^{-(R_0/2)\xi}}{\nu_0}\frac{\partial(\psi,e^{(R_0/2)\xi}W)}{\partial(\xi,\eta)}+R_0\frac{\partial W}{\partial\xi}+\left(\frac{R_0}{2}\right)^2 W. \tag{10}$$

Note that, via Eq. (2), the first term on the right-hand side gives a quasilinear coupling to the flow field. This coupling also constitutes an unavoidable nonlinearity.

To examine Eq. (10) on $\mathcal{D}_{\xi,\eta}$, first consider a uniform background zonal flow in ζ-coordinates,

$$\vec{q}_0=(-\partial_y\psi_0,\partial_x\psi_0),\psi_0(\xi,\eta)=-U_0h\,\eta(x,y), \tag{11}$$

where the magnitude of the mean flow speed U_0 is constant. Substituting ψ_0 for ψ in Eq. (10) and taking $W(\xi,\eta)$ to be time independent, we obtain a linear eigenvalue equation,

$$-\Delta_{\xi,\eta}W+(i\lambda/J)W=-(R_0/2)^2W. \tag{12}$$

This is a Schrödinger-type equation that we will hereafter refer to as the Schrödinger-vorticity equation. The real part of $i\lambda$ must be negative, by positivity of J. The real part of $\nu_0\lambda$ gives the frequencies that we will study below. Of course, the vorticity amplitude W must satisfy boundary conditions on $\partial\mathcal{D}_{\xi,\eta}$ and as $\xi\to\pm\infty$.

To model the vorticity near a boundary layer we impose the conditions $\partial_\eta W(\xi,\pm1)=0$ and $|W|\to0$ as $|\xi|\to\infty$. To obtain the modified flow field $\psi_0+\psi_1$ we also need to solve, from Eqs. (2), (9), and (11), the Poisson equation,

$$\Delta_{\xi,\eta}\psi_1=(1/J)e^{(R_0/2)\xi}W(\xi,\eta), \tag{13}$$

with the imposed boundary conditions, $\psi_1(\xi,\pm1)=0$ and $|\psi_1|\to0$ as $|\xi|\to\infty$, to ensure that no new fluid flows into the domain. In obtaining Eq. (13), the time dependence $e^{i\lambda\nu_0 t}$ is ignored, assuming that a steady state has been reached for W.

Consider $i\lambda\in\mathbf{R}$ and define the bound-states potential,

$$V_b(\xi,\eta)\equiv 1/[h^2J(\xi,\eta)]-1, \tag{14}$$

which is smooth and short-ranged, i.e., $|V_b|=\mathcal{O}(|\xi|^{-2})$ for large $|\xi|$. Substituting (14) into Eq. (12) the Schrödinger-vorticity equation becomes

$$-\Delta_{\xi,\eta}W+(i\lambda h^2)V_b(\xi,\eta)W=-[i\lambda h^2+(R_0/2)^2]W. \tag{15}$$

For square-integrable eigenfunctions W in Eq. (15), $i\lambda$ must be in the interval $(-(R_0/2h)^2,0)$. Then, by standard self-adjoint operator theory, eigenvalues will exist for R_0 and $-i\lambda$ real, positive and sufficiently large [7].

Solving for the eigenvalues of Eq. (15) with spectral methods is now straightforward. To study basic physical aspects of this equation, we assume a thin channel and express the approximate eigensolution as $W(\xi,\eta)=W_*\Phi_b(\xi)\sin(\pi\eta/2)$ with normalization condition: $\max\{\Phi_b\}=1$. The midchannel double-well potential is defined to be $U_b(\xi)\equiv-V_b(\xi,0)$. Example profiles are plotted in Fig. 2.

Equation (15) is now a 1D eigenvalue problem:

$$-\Phi_b''(\xi)+\lambda_bU_b(\xi)\Phi_b(\xi)=E_b\Phi_b(\xi), \tag{16}$$

where $\lambda_b\equiv-i\lambda h^2$ and $E_b\equiv\lambda_b-(\pi/2)^2-(R_0/2)^2$. We solve for the (symmetric) ground state, with (negative) eigenvalue E_b, using matrix elements. The Reynolds number is then given by the expression $R_0=2\sqrt{\lambda_b-E_b-(\pi/2)^2}$. Determining the coupling parameter λ_b from R_0 is well-defined, but not explicit.

From the Poisson equation (13) we obtain $\psi_1(\xi,\eta)$. It is because of the translation factor $e^{(R_0/2)\xi}$ that separation occurs downstream. Figure 3 indeed shows how, after passing over the stenosis, there is a separation of the vortex from the downstream flow. Such separation occurs only for sufficiently large W_*. The parameter $W_*=\max|e^{(-R_0/2)\xi}\omega(x,y,0)|$ represents the maximal outer wall stress which occurs a little distance downstream from the peak of the stenosis [6].

Using a numerical shooting program [8] we simulated Eqs. (1) and (2). The spectral method, cf. Eqs. (13) and (15), was used to obtain stationary solutions. Results are depicted in Figs. 3 and show good agreement.

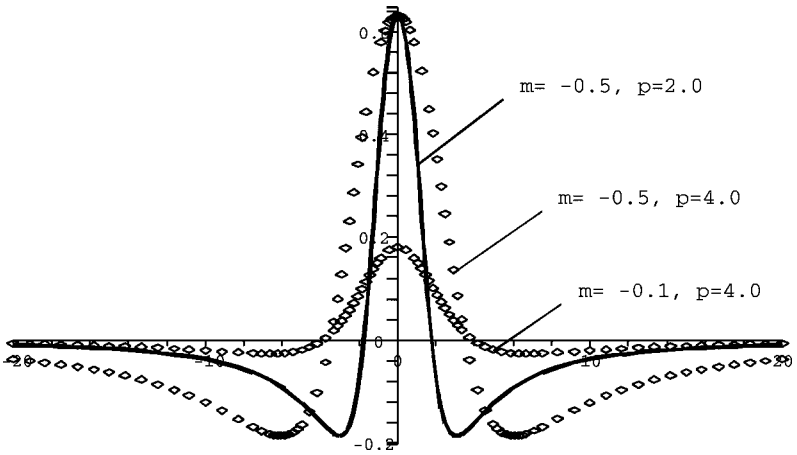

FIG. 2. The shape of the midchannel potential $U_b(\xi)$ for a boundary with stenosis.

Figure 2 represents the potential in the middle of the channel. From Eq. (14) it can be seen that the wells get deeper when moving away from the middle of the channel. The ground state thus gets pushed towards the boundaries and that is why a stable stationary vortex materializes.

For the study of traveling vortices we reconsider the Schrödinger vorticity equation (12) with the assumption that $\mathrm{Re}(i\lambda)<0$ and $\mathrm{Im}(i\lambda)>0$, and use a decomposition of the vorticity amplitude in a neighborhood of the saddle point (0,0) for the Jacobian J. Numerical solutions suggest a separation of variables in the form $W(\xi,\eta)=\Phi_r(\xi)\sinh(B_r\eta)+\delta W(\xi,\eta)$ [9]. Here B_r is a slip parameter for the perturbed contribution to the flow, i.e., $B_r\to 0^+$ for nearly parabolic profiles, whereas $B_r\to+\infty$ for negligible boundary shear stress flows. Making the substitution into Eq. (12) and neglecting δW leads to a 1D complex eigenvalue problem for $\Phi_r(\xi)$. Indeed, for $m<0$, define the resonance potential:

$$V_r(\xi,\eta)\equiv 1/[h^2J(\xi,\eta)]-e^{-2|m|}, \tag{17}$$

with $h^2J(0,0)=e^{2|m|}$. We are led to the eigenvalue equation,

$$-\Delta_{\xi,\eta}W+i\lambda h^2V_r(\xi,\eta)W=\mathcal{E}_rW, \tag{18}$$

where $\mathcal{E}_r\equiv -i\lambda h^2e^{-2|m|}-(R_0/2)^2$ is a complex eigenvalue. Note that the resonance potential has a saddle-point at (0,0) where $V_r=0$. In particular, the behavior near the origin is

$$V_r(\xi,\eta)=A_r\xi^2-A_r\eta^2+\mathcal{O}(\xi^4,\xi^2\eta^2,\eta^4),$$
$$A_r\equiv 6|m|h^2/(e^{2|m|}p^2). \tag{19}$$

Here A_r is a concavity parameter for V_r. For the shallow perturbations (cf. Eq. (6)) we have $A_r\simeq p^2\kappa^2/(6|m|)\simeq(h/e^{|m|})|\kappa|\simeq y_0|\kappa|$ for $p\gg y_0$. The quantity $y_0|\kappa|$ characterizes the perturbation in that it is the ratio of the cross-sectional width and the radius of curvature.

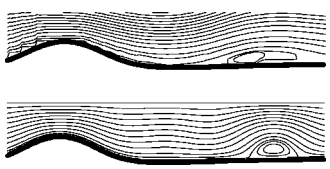

FIG. 3. Numerically computed stream function [8] for $m=-0.5$, $p=2$, $U_0=1.0$, $R_0=500$, and Prandtl number=1.0 (top). Theoretical stream function from spectral method for $m=-0.5$, $p=2$, $U_0=1.0$, $R_0=500$, and $W_*=0.22$ (bottom).

To asymptotically solve Eq. (18) let $\Phi_r(\xi)\simeq W_{**}\phi(\xi)$, where $\phi(\xi)$ solves the 1D eigenvalue equation:

$$-\phi''+i\lambda h^2A_r\xi^2\phi=[B_r^2+\mathcal{E}_r]\phi, \tag{20}$$

with normalization $\int_{-\infty}^{\infty}|\phi|^2d\xi=1$, so that W_{**} is the steady state amplitude of the disturbance. The harmonic oscillator problem in Eq. (20) has no solution if $\mathrm{Im}(i\lambda)\neq 0$. To obtain square integrable solutions we need to scale the spatial coordinates: $\xi\to e^{\theta}\xi$, $\partial_\xi\to e^{-\theta}\partial_\xi$ for complex θ [10]. The function ϕ and its derivatives are changed from ϕ, ϕ', and ϕ'' to $\phi_\theta=e^{\theta/2}\phi(e^\theta\xi)$, $\phi'_\theta=e^{-\theta/2}\phi'(e^\theta\xi)$, and $\phi''_\theta=e^{-3\theta/2}\phi''(e^\theta\xi)$, respectively. To facilitate the discovery of solutions, write $i\lambda=-\lambda_re^{-i\beta_r}$, where the quantities $\lambda_r\in\mathbf{R}^+$ and $\beta_r\in(0,2\pi)$ are to be determined by the scaled eigenvalue problem. From Eq. (20) we find

$$-e^{-2\theta}\phi''_\theta+i\lambda h^2A_re^{2\theta}\xi^2\phi_\theta=[B_r^2+\mathcal{E}_r]\phi_\theta. \tag{21}$$

An optimal choice for the complex-variable rotation is $\theta=i(\beta_r+\pi)/4$. Indeed, multiplying Eq. (21) by $e^{2\theta}\phi_\theta^*$ and then integrating in ξ over $(-\infty,\infty)$ gives

$$\int_{-\infty}^{\infty}|\phi'_\theta|^2d\xi+\lambda_rh^2A_r\int_{-\infty}^{\infty}|\xi\phi_\theta|^2d\xi$$
$$=i[e^{i\beta_r/2}B_r^2+\lambda_re^{-i\beta_r/2}h^2e^{-2|m|}-e^{i\beta_r/2}(R_0/2)^2]. \tag{22}$$

Here we normalize with $\int_{-\infty}^{\infty}|\phi_\theta|^2d\xi=1$. Requiring the imaginary part of Eq. (22) to vanish and assuming $\cos(\beta_r/2)\neq 0$ leads to an identity involving the eigenvalue, the Reynolds number and the slip parameter:

$$\lambda_r=[(R_0/2)^2-B_r^2]e^{2|m|}/h^2. \tag{23}$$

Hence the angular frequencies $\nu_0\lambda$ in Eq. (9) are restricted to a circle of radius $\nu_0\lambda_r$ in the complex plane.

Finally, define the parameter $\mu_r>0$ so that $\mu_r^4=[(R_0/2)^2-B_r^2]e^{2|m|}A_r$. Then the eigensolutions ϕ_θ of Eq. (21) are Hermite functions with eigenvalues,

$$\mu_r^2(2k+1)=[\lambda_rh^2e^{-2|m|}+(R_0/2)^2-B_r^2]\sin(\beta_r/2), \tag{24}$$

with $k=0,1,2,\ldots$, from which we can solve for $\sin(\beta_r/2)$ and obtain, using Eq. (23), the discrete family,

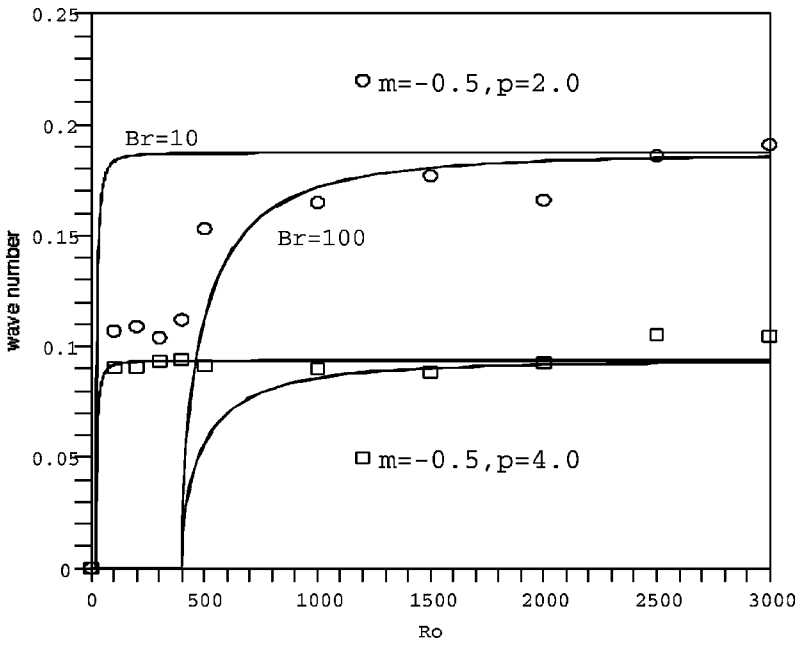

FIG. 4. Wave number f/U_0 versus Reynolds number R_0: theoretical—; from top to bottom: numerical $(m,p)=\circ(0.5,2.0)$, $\square$ (0.5, 4.0). For Reynolds numbers smaller than about 500, it is the stronger damping that affects the validity of our approximations.

$$\beta_r \to \beta_{r,k} \equiv 2\ \arcsin\left(\frac{\sqrt{A_r}e^{2|m|}(2k+1)}{2\sqrt{\lambda_r}h}\right). \tag{25}$$

Note that there are no traveling vortices if λ_r is negative, or if $A_r > 4\lambda_r h^2/e^{4|m|}$. These restrictions, together with Eq. (23), lead to the condition $R_0 \geqslant \sqrt{e^{2|m|}A_r + 4B_r^2}$ for the formation of traveling vortices. Thus, increasing the boundary slip B_r suppresses the formation of fluid waves. In other words, in a well lubricated channel no traveling vortices occur. Also, as the curvature of the perturbation, measured in part by A_r, is increased, the oscillations are initiated only for sufficiently large R_0. For the $k=0$ complex frequency we find

$$i\lambda = -[(R_0/2)^2 - B_r^2](e^{2|m|}/h^2) \times \exp\left[-i2\ \arcsin\left(\frac{e^{|m|}}{2}\sqrt{\frac{A_r}{(R_0/2)^2 - B_r^2}}\right)\right]. \tag{26}$$

The imaginary part of this expression, $\mathrm{Im}(i\lambda)=\mathrm{Re}(\lambda)$, is found to be

$$\mathrm{Re}(\lambda) = \frac{e^{3|m|}}{2h^2}\sqrt{A_r}\sqrt{R_0^2 - 4B_r^2 - e^{2|m|}A_r}. \tag{27}$$

For the Strouhal frequency, $f=\nu_0\,\mathrm{Re}(\lambda)/2\pi$ (see, e.g., Ref. [8]), we now have the following expression:

$$f = \frac{\sqrt{6}}{4\pi}\frac{U_0\sqrt{|m|}e^{2|m|}}{p}\left(1 - \frac{4B_r^2p^2 + 6|m|h^2}{R_0^2p^2}\right)^{1/2}. \tag{28}$$

The coefficient $\sqrt{|m|}e^{2|m|}/p$ is a shape-size parameter that approximately equals $\sqrt{6\kappa h}$. The coefficient $\sqrt{6}/4\pi \simeq 0.195$ is called the Strouhal number and is typically obtained from experimental observations. It is, for instance, found to be 0.212 for uniform flow around a cylindrical obstacle [8]. All else being equal, the wave number f/U_0 is constant at large R_0, cf. Fig. 4.

We conclude that oscillations will occur only for $A_r > 0$ and $R_0 > \sqrt{e^{2|m|}A_r + 4B_r^2}$. In particular, for the case of no slip ($B_r=0$), any $R_0 > e^{|m|}\sqrt{A_r}$ will produce waves for any perturbation $A_r > 0$. However, the frequency vanishes as $A_r \to 0^+$. Conversely, in the case of negligible boundary shear stress, i.e., near perfect slip ($B_r \to +\infty$), a very high Reynolds number is required to initiate oscillations.

Cardiac physiologists have been aware for centuries that murmurs (also known as "bruits") occur in arteries with a sufficiently large stenosis [11]. To our knowledge, the above results constitute the first analytical description, based on elementary fluid mechanics, for how such murmurs arise.

M.B. thanks the Eppley Foundation for funding.

[1] P. S. Marcus, J. Fluid Mech. **215**, 393 (1990).
[2] M. E. Goldstein, *Aeroacoustics* (McGraw-Hill, New York, 1976).
[3] C. G. Caro *et al.*, *The Mechanics of the Circulation* (Oxford University Press, Oxford, 1978).
[4] W. Liao *et al.*, Comments Mod. Phys., Part C **14**, 635 (2003).
[5] T. B. Moodie *et al.*, Acta Mech. **54**, 107 (1984).
[6] K. B. Ranger and H. Brenner, J. Fluid Mech. **152**, 1 (1985).
[7] M. Reed and B. Simon, *Methods of Modern Mathematical Physics IV* (Academic Press, New York, 1978).
[8] M. Griebel *et al.*, *Numerical Simulation in Fluid Dynamics: A Practical Introduction* (SIAM Monographs, Philadelphia PA, 1997).
[9] S. Chen *et al.*, Phys. Rev. Lett. **81**, 5338 (1998).
[10] P. Briet *et al.*, Commun. Partial Differ. Equ. **12**, 201 (1987).
[11] P. May *et al.*, J. Vasc. Res. **39**, 21 (2002).